Inorganic Chemistry
Article

Inorg. Chem. **2009**, *48*, 5449–5453 **5449**
DOI: 10.1021/ic900504m

Synthesis and Characterization of a Fluorotitanophosphate $(NH_4)_{0.16}K_{1.84}[Ti_2F_2(PO_4)_2(PO_3OH)]$ with a Unique Lamella Framework

Sihai Yang,[†] Guobao Li,*[,†] Wei Liu,[‡] Wei Wang,*[,‡] Zhimin Yan,[§] Yining Huang,*[,§] Fuhui Liao,[†] and Jianhua Lin*[,†]

[†]*Beijing National Laboratory for Molecular Sciences (BNLMS), State Key Laboratory of Rare Earth Materials Chemistry and Applications, College of Chemistry and Molecular Engineering, Peking University, Beijing 100871, P. R. China,* [‡]*State Key Laboratory of Applied Organic Chemistry, College of Chemistry and Chemical Engineering, Lanzhou University, Gansu 730000, P. R. China, and* [§]*Department of Chemistry, The University of Western Ontario, London, Ontario, Canada N6A 5B7*

Received March 14, 2009

$(NH4)_{0.16}K_{1.84}[Ti_2F_2(PO_4)_2(PO_3OH)]$ (**1**) has been synthesized under hydrothermal conditions. The structure, the composition, and the thermal stability of **1** were determined by single-crystal X-ray diffraction; inductively coupled plasma−optical emission spectroscopy; IR spectroscopy; elemental analysis; thermogravimetric analysis−differential scanning calorimetry−mass spectrometry; and solid-state ^1H, ^{31}P, and ^{19}F NMR, and the phase purity of the bulk sample was checked by powder X-ray diffraction. Complex **1** is a fluorotitanophosphate having a unique lamella framework with both TiO_5F octahedra and PO_3OH tetrahedra on the surface of the layer, which leads to two different hydrogen bondings involving both P−OH and Ti−F groups.

Introduction

During the past several decades, titanium phosphates with a lamella structure have been extensively studied due to their intercalation chemistry,[1] ion exchange applications,[2] and catalytic properties.[3] Although several lamella titanium phosphates with different layered structures have been reported, the types of the titanium phosphate layers are still limited. The most important members of titanium phosphates include α-TiP (α-$Ti(HPO_4)_2\cdot H_2O$[4]), γ-TiP (γ-$Ti(H_2PO_4)(PO_4)\cdot 2H_2O$,[5] and its anhydrous phase β-$Ti(H_2PO_4)(PO_4)$[6]). The intercalation chemistry of these materials stems from the presence of medium−strong P−OH Brønsted acid groups located on the surfaces of the interlayer region. Recently, a different type of layered titanium phosphate, $Ti_2(PO_4)_2F_4\cdot N_2C_2H_{10}$, was reported among several fluoro-substituted titanophosphates.[7] The layer in this compound is built upon the alternative linkages between TiO_4F_2 octahedra and PO_4 tetrahedra. This titanium phosphate exhibits different intercalation chemistry from that of α- and γ-TiP, since the Ti−F bonds are oriented perpendicularly to the layer, resulting in strong hydrogen bonding with amino groups or water molecules to stabilize the overall framework structure. Our research is focused on designing new titanium-phosphate-based lamellar materials with high stability and novel intercalating properties. We report here the synthesis and characterization of a novel fluoro-substituted titanophosphate, $(NH_4)_{0.16}K_{1.84}[Ti_2F_2(PO_4)_2(PO_3OH)]$ (**1**), with a unique lamella structure, which offers both P−OH and Ti−F groups on the layer surfaces for potential hydrogen bonding with guest molecules.

Experimental Section

Synthesis. Complex **1** was synthesized hydrothermally. A typical example was to charge a mixture of K_2TiF_6 (12.5 mmol), H_3PO_4 (130 mmol), and $N_2H_4\cdot H_2O$ (35 mmol) in a 50 mL

*To whom correspondence should be addressed. Tel.: (8610)62750342. Fax: (8610)62753541. E-mail: liguobao@pku.edu.cn (G.L.), Wang_wei@lzu.edu.cn (W.W.), yhuang@uwo.ca (Y.H.); jhlin@pku.edu.cn (J.L.).

(1) Mafra, L.; Rocha, J.; Fernandez, C.; Castro, G. R.; Garcia-Granda, S.; Espina, A.; Khainakov, S. A.; García, J. R. *Chem. Mater.* **2008**, *20*, 3944.
(2) Parida, K. M.; Sahu, B. B.; Das, D. P. *J. Colloid Interface Sci.* **2004**, *270*, 436.
(3) Das, D. P.; Parida, K. M. *J. Mol. Catal. A: Chem.* **2007**, *276*, 17.
(4) (a) Nunes, L. M.; Airoldi, C. *J. Solid State Chem.* **2000**, *154*, 557. (b) Nunes, L. M.; Airoldi, C. *Mater. Res. Bull.* **1999**, *34*, 2121. (c) Espina, A.; Garcia, J. R.; Guil, J. M.; Jaimez, E.; Parra, J. B.; Rodriguez, J. *J. Phys. Chem.* **1998**, *102*, 1713. (d) Salvado, M. A.; Pertierra, P.; Garcia-Granda, S.; Garcia, J. R.; Rodriguez, J.; Fernandez-Diaz, M. T. *Acta Crystallogr.* **1996**, *B52*, 896. (e) Airoldi, C.; De Oliveira, S. F. *Struct. Chem.* **1991**, *2*, 41.
(5) (a) Mafra, L.; Paz, F. A. A.; Rocha, J.; Espina, A.; Khainakov, S. A.; Garcia, J. R.; Fernandez, C. *Chem. Mater.* **2005**, *17*, 6287. (b) Chen, C.; Yang, Y. L.; Huang, K. L.; Sun, Z. H.; Wang, W.; Yi, Z.; Liu, Y. L.; Pang, W. Q. *Polyhedron* **2004**, *23*, 3033. (c) Christensen, A. N.; Andersen, E. K.; Andersen, I. G. K.; Alberti, G.; Nielsen, M.; Lehmann, M. S. *Acta Chem. Scand.* **1990**, *44*, 865.
(6) Andersen, A. M. K.; Norby, P.; Vogt, T. *J. Solid State Chem.* **1998**, *140*, 266.
(7) (a) Yang, S. H.; Li, G. B.; Blake, A. J.; Sun, J. L.; Xiong, M.; Liao, F. H.; Lin, J. H. *Inorg. Chem.* **2008**, *47*, 1414. (b) Yang, S. H.; Li, G. B.; You, L. P.; Tao, J. L.; Loong, C. K.; Tian, S. J.; Liao, F. H.; Lin, J. H. *Chem. Mater.* **2007**, *19*, 942. (c) Yang, S. H.; Li, G. B.; Li, L.; Tian, S. J.; Liao, F. H.; Xiong, M.; Lin, J. H. *Inorg. Chem.* **2007**, *46*, 11431. (d) Serre, C.; Taulelle, F.; Ferey, G. *Chem. Mater.* **2002**, *14*, 998. (e) Fu, Y. L.; Liu, Y. L.; Shi, Z.; Zou, Y. C.; Pang, W. Q. *J. Solid State Chem.* **2001**, *162*, 96. (f) Serre, C.; Férey, G. *J. Mater. Chem.* **1999**, *9*, 579.

Published on Web 05/18/2009

Teflon-lined stainless steel autoclave. The autoclave was sealed and heated to 200 °C at a rate of 5 °C/h. It was kept at 200 °C under autogenous pressure for 25 days and then cooled to room temperature at a rate of 5 °C/h. The colorless crystalline product was filtered, washed with hot distilled water, and dried at ambient temperature to give about 1.5 g of the product (yield 50% based on K_2TiF_6).

Characterization. Powder X-ray diffraction (PXRD) data were collected on a Bruker D8 Advance diffractometer with Cu Kα1 (λ = 1.54056 Å) radiation (2θ range, 7−120°; step, 0.0197°; scan speed, 30 s/step) at 50 kV and 40 mA. PXRD patterns were refined from single-crystal data using GSAS[8] software. During the refinement, the parameters for the lattice, background, and peak profile were refined; however, the atom fraction coordinates were the same as obtained from single-crystal data. The refined patterns closely matched those obtained from the bulk sample, as shown in Figure 1, indicating that a large amount of pure compounds can be obtained. IR spectra were recorded in the 400−4000 cm^{-1} range using a Magna-IR 750 FTIR spectrometer. All NMR experiments were performed on a Varian/Chemagnetics InfinityPlus 400 WB spectrometer equipped with three rf channels. At a field strength of 9.4 T, the resonance frequencies are 399.493, 375.863, and 161.719 MHz for ^1H, ^{19}F, and ^{31}P, respectively. The ^{19}F and ^{31}P shifts were referenced to $CFCl_3$ and 85% H_3PO_4. A 5 mm H/F/X triple-tuned magic angle spinning (MAS) probe was used to obtain ^{19}F and ^{31}P spectra. The $\pi/6$ flip angles of 2 and 3 μs were used for ^{19}F and ^{31}P. The pulse delay was 10 and 60 s for ^{19}F and ^{31}P. For rotational echo double resonance (REDOR) experiments, a standard REDOR pulse sequence was employed.[9] The $\pi/2$ pulse of ^{31}P and π pulse of ^{19}F were 6 and 10 μs. A pulse delay of 240 s and a spinning rate of 10 kHz were utilized. The elemental ratio (K/Ti/P) of **1** was measured by inductively coupled plasma−optical emission spectroscopy (ICP-OES) on a Varian Vista RL spectrometer with radial plasma observation. As a typical analytical process, **1** was dissolved in acid (HCl and HNO_3) to an appropriate concentration and then measured by ICP-OES in three parallel samples, which resulted in an average K/Ti/P ratio of 1.84:1.92:3.00. A thermogravimetric analysis−differential scanning calorimetry−mass spectrometry (TG-DSC-MS) analysis was performed at a heating rate of 10 °C/min using a NETZSCH STA449C instrument. Elemental analyses were carried out on an Elementar Vario EL III microanalyzer. Anal. calcd for **1**: N, 0.45; H, 0.33. Found: N, 0.40; H, 0.73 (a background of about 0.5 for H was found even though there was no hydrogen in the sample).

Crystallographic Study. A small single crystal of **1** (colorless, dimensions about 0.1 × 0.1 × 0.15 mm) was carefully selected under an optical microscope and glued to thin glass fibers with epoxy resin. Intensity data were collected on a Bruker SMART X-ray diffractometer, equipped with an APEX-CCD area detector and using graphite-monochromatic Mo Kα (λ = 0.71073 Å) radiation at room temperature. The data absorption correction was applied on the basis of symmetry-equivalent reflections using the ABSOR program.[10] The structure was solved with direct methods and refined on F^2 with full-matrix least-squares methods using the SHELXS-97 and SHELXL-97 programs,[11] respectively. All nonhydrogen atoms were refined anisotropically. The hydrogen atoms were added to the riding model and refined isotropically with N−H = 0.850 Å and O−H = 0.820 Å. The occupancy of N was fixed at the analytical value of the nitrogen element. The crystallographic data and the structural refinement parameters are summarized in Table 1. The corresponding bond lengths are listed in Table 2 (the atomic positions are listed in the Supporting Information). Further details of the crystal structure reported in this paper can be obtained from the Fachinformationszentrum Karlsruhe, 76344 Eggenstein-Leopoldshafen, Germany, (fax, (49) 7247 808 666; e-mail, crysdata@fiz-karlsruhe.de) on quoting the depository number CSD-420490.

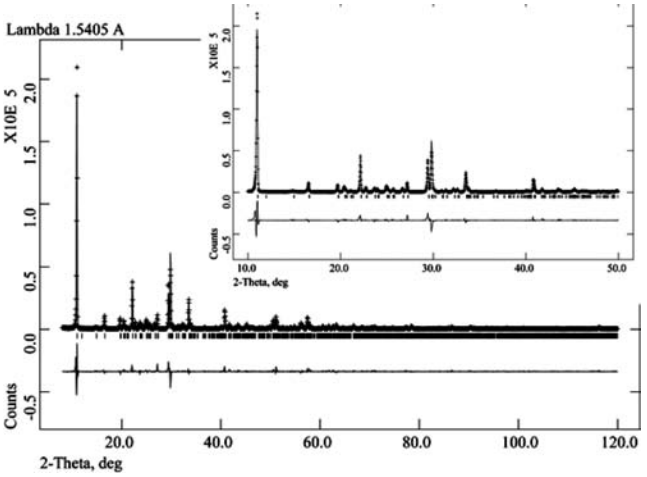

Figure 1. Powder diffraction patterns and the Rietveld plots for **1**. The symbol + represents the observed value. The solid line represents the calculated value. The marks below the diffraction patterns are the calculated reflection positions, and the difference curve is shown at the bottom of the figure.

Table 1. Crystallographic and Structural Refinement Parameters for **1**

formula	$(NH_4)_{0.16}K_{1.84}$-$[Ti_2F_2(PO_4)_2$-$(PO_3OH)]$	Z	4
fw	494.55	d_{calcd} ($g\cdot cm^{-3}$)	2.799
space group	$C2/c$	λ (Mo Kα) (Å)	0.71073
a (Å)	16.406(3)	GOF on F^2	1.000
b (Å)	8.323(2)	μ (mm^{-1})	2.515
c (Å)	8.826(2)	R_{int}	0.0242
β (deg)	103.16(3)	R1, wR2 ($I > 2\sigma(I)$)	0.0310, 0.0780
V ($Å^3$)	1173.5(4)	R1, wR2 (all data)	0.0381, 0.0815

Table 2. Selected Bond Distances (Angstroms) for **1**

bond	length (Å)	bond	length (Å)	bond	length (Å)
Ti1−F1	1.883(1)	Ti1−O5	1.930(1)	P2−O1	1.529(2)
Ti1−O1	1.915(1)	Ti1−O6	1.911(1)	P2−O2	1.526(2)
Ti1−O2	1.888(2)	P1−O5 × 2	1.521(2)	P2−O3	1.534(2)
Ti1−O4	1.947(1)	P1−O6 × 2	1.520(1)	P2−O4	1.525(1)

Results

Infrared (IR) Spectra. The Fourier transform infrared (FTIR) microspectroscopy results of **1** are shown in Figure 2. The strong bands at about 1218 and 1024 cm^{-1} originate from tetrahedral phosphate PO_4.[12] The bands at 3238 and 1426 cm^{-1} can be attributed to the vibrations of NH_4^+.[12]

Structure Description. The crystal structure of **1** adopts a 2-D lamella structure. In the asymmetric unit (Figure 3),

(8) (a) Larson, A. C.; von Dreele, R. B. *Report LAUR 86-748*, Los Alamos National Laboratory, Los Alamos, NM, **1985**. (b) Rietveld, H. M. *J. Appl. Crystallogr.* **1969**, *2*, 65.

(9) Gullion, T.; Schaefer, J. *J. Magn. Reson.* **1989**, *81*, 196.

(10) Higashi, T. *ABSCOR, Empirical Absorption based on Fourier Series Approximation*; Rigaku Corporation: Tokyo, **1995**.

(11) (a) Sheldrick, G. M. *SHELXS97*; University of Göttingen: Göttingen, Germany, **1997**.(b) Sheldrick, G. M. *SHELXL97*; University of Göttingen: Göttingen, Germany, **1997**.

(12) Birsöz, B.; Baykal, A.; Toprak, M.; Köseoglu, Y. *Cent. Eur. J. Chem.* **2007**, *5*, 536–545.

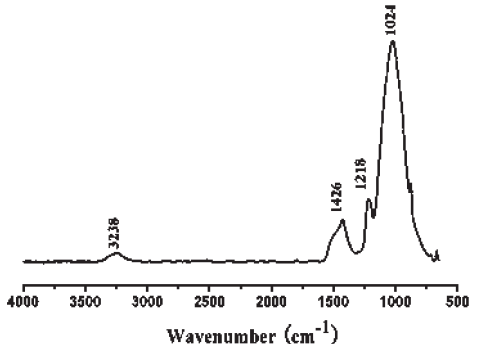

Figure 2. FTIR spectra of **1**.

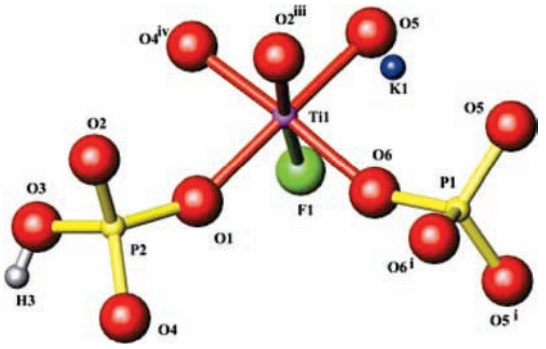

Figure 3. Asymmetric unit of **1**. Symmetry code: (i) $-x$, y, $-3/2 - z$; (ii) $-x$, $-1 - y$, $-1 - z$; (iii) $-x$, $-y$, $-1 - z$; (iv) x, $-y$, $1/2 + z$.

there are 12 crystallographically independent atoms, including one K (with an occupancy of 0.92) or NH_4 group (with an occupancy of 0.08), one Ti, six O's, two P's, one F, and one H (with an occupancy of 0.5). The titanium atom is coordinated to five bridging oxygen atoms and one terminal fluorine atom to form a TiO_5F octahedron. The bond lengths of Ti−O (ranging from 1.888 to 1.947 Å) and Ti−F (1.883 Å) are consistent with those reported in the literature.[4−7] The coordination environments of the two phosphorus sites (P1 and P2) with a ratio of 1:2 are different from each other. P1 is bonded to four bridging oxygen atoms (O5, O6, O5^{i}, and O6^{i}) to form a PO_4 tetrahedron, while P2 is connected to three bridging oxygen atoms (O1, O2, and O4) and one terminal oxygen atom or a hydroxyl group to form a mixture of equally occupied PO_4 and PO_3OH tetrahedra.

The TiO_5F octahedra are not directly connected to each other; they are connected to the PO_4 or PO_3OH tetrahedra via corner-sharing to form anionic $[Ti_2F_2(PO_4)_2(PO_3OH)]^{2-}$ layers. Figure 4 shows the network structure of the layer, where oxygen, fluorine, and hydrogen atoms are omitted for clarity. This layer contains folding ladders formed by TiO_5F octahedra and $P2O_4$ or $P2O_3OH$ tetrahedra (emphasized by blue lines), which are further connected by $P1O_4$ tetrahedra (expressed as green lines). This is a unique titanium phosphate layer, in which the $P1O_4$ tetrahedra are located at the middle and are sandwiched by TiO_5F octahedra and $P2O_4$ or $P2O_3OH$ tetrahedra. Therefore, the terminal atoms (F1, O3, or O3H) are exposed to the surface, resulting in strong

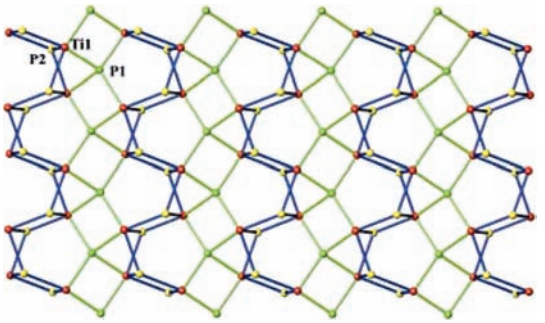

Figure 4. The layer structure of **1**. The Ti atoms are in red, P2 in yellow, and P1 in green. The connections of folding ladders are in blue, and the connections with P1 tetrahedra are in green.

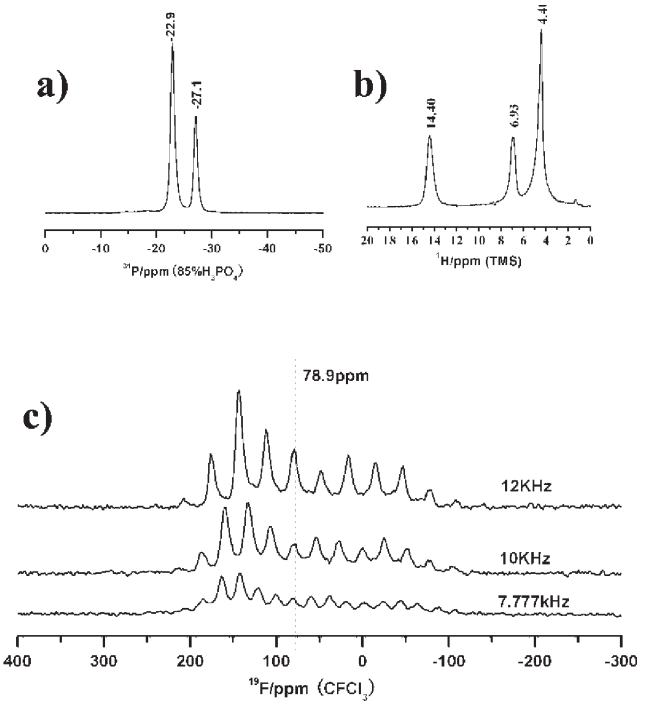

Figure 5. (a) ^{31}P MAS NMR spectrum of **1**. (b) ^{1}H MAS NMR spectrum of **1**. (c) ^{19}F MAS NMR spectra of **1** with three spinning rates.

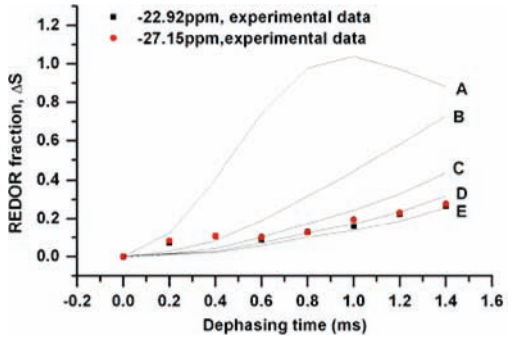

Figure 6. Calculated REDOR curves corresponding to an average P−F dipolar coupling of (A) 1696.8 Hz (r_{PF} = 3.0 Å), (B) 715.84 Hz (r_{PF} = 4.0 Å), (C) 502.76 Hz (r_{PF} = 4.5 Å), (D) 414.26 Hz (r_{PF} = 4.8 Å), and (E) 366.51 Hz (r_{PF} = 5.0 Å).

hydrogen bonding (O3−H3···O3) between the layers, which is very similar to that found in $HCoO_2$.[13]

NMR Spectra. The ^{31}P solid-state MAS NMR spectrum (Figure 5) exhibits two resonance signals at −22.9 and −27.1 ppm with a 2:1 intensity ratio, indicating the

(13) (a) Delaplane, R. G.; Ibers, J. A.; Ferraro, J. R.; Rush, J. J. *J. Chem. Phys.* **1969**, *50*, 1720. (b) Emsley, J. *Chem. Soc. Rev.* **1980**, *9*, 91.

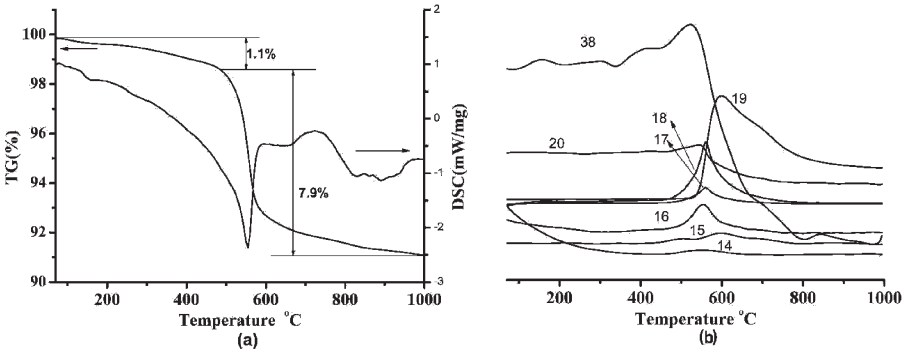

Figure 7. TG-DSC-MS curves for **1**.

presence of two nonequivalent P sites in the structure.[7a,14] The NMR result confirms the X-ray structure, showing that there are two crystallographically distinct P sites with a 2:1 ratio in the asymmetric unit of **1**. On the basis of the chemical shift and the relative intensity ratio, the two peaks at −22.9 and −27.1 ppm in the ^{31}P MAS spectrum can be assigned to P2 and P1, respectively. ^{19}F solid-state MAS NMR spectra obtained at three spinning speeds are shown in Figure 5c. Only the position of the peak at 78.9 ppm did not change with the spinning speed, indicating that there is only one crystallographically distinct F atom in the asymmetric unit, and its isotropic chemical shift is 78.9 ppm. The large number of spinning sidebands indicates that the F has large chemical shift anisotropy.

To probe the spatial relationship between P and F atoms, we also carried out ^{31}P{^{19}F} REDOR experiments. REDOR is a rotor-synchronized MAS experiment. It is designed to measure the heteronuclear dipolar interaction and therefore provides P−F distance information (Figure S1 in Supporting Information shows the typical ^{31}P{^{19}F} REDOR spectra with short, medium, and long dephasing times.). Observing both P sites in REDOR difference spectra suggests that both P sites are dipolar coupled to the F. However, the coupling is fairly weak since the REDOR difference signals of both P's are very weak (especially in the spectra with short dephasing times). This result implies a relatively long P−F distance. Figure 6 shows the plots of the REDOR fraction as a function of the dephasing time, revealing that both P sites dephase at the same rate, implying that the strength of the dipolar coupling between F and P is the same for both P sites. The REDOR simulations (Figure 6) indicate that the average P−F distances are about 4.8 Å, which suggests that the F is not directly bonded to any P. This agrees well with the X-ray structure, which shows that the F is only directly bonded to Ti and the P−F distances are about 4.0 Å. In the ^{1}H MAS NMR spectrum (Figure 4b), three resonances were observed. The resonance at 4.4 ppm originates from physically absorbed water,[15] whereas the peak at 14.4 ppm may be attributed to the protons in the PO_3OH group.[15] The signal at 6.93 ppm can be assigned to the protons of the NH_4 group.[15] The highly deshielded proton chemical shift of the PO_3OH group suggests that the proton in this group is highly acidic. Thus, this material may potentially be used as a strong solid acid for catalysis.

Thermal Properties. The TG-DSC-MS curves of **1** under an argon atmosphere are shown in Figure 7. Compound **1** gradually loses mass (about 1.1 wt %) up to 500 °C, and then a dramatic mass loss occurs at around 550 °C. According to the mass spectra shown in Figure 7b, the observed species with m/z values of 14, 15, 16, 17, 18, 19, 20, and 38 can be assigned to N, NH, NH_2 (or O), OH (or NH_3), H_2O, F, HF, and F_2, respectively. The release of the above species was not found until the temperature reached 500 °C. Therefore, the weight loss from room temperature to about 500 °C may be attributed to the deviation of the baseline. The large mass loss of 7.9% at around 550 °C is likely due to the complete decomposition of compound **1** to $KTi_2(PO_4)_3$, $KTiOPO_4$, and TiO_2 (the calculated mass loss is about 7.5%), which were identified by powder X-ray diffraction (see Figure 8b). The X-ray diffraction patterns of **1** treated from 220 to 1000 °C were shown in Figure 8a. The X-ray diffraction patterns did not change until 400 °C, which indicated that **1** is stable below 400 °C.

Discussion and Conclusion

In Figure 9, we compare several representative layers in titanium phosphates reported in the literature. The layers of α-TiP and γ-TiP are constructed by corner-sharing of TiO_6 octahedra and PO_4, PO_3OH, or $PO_2(OH)_2$ tetrahedra (additional drawings can be seen in Figure S2 in Supporting Information). The TiO_6 octahedra and PO_4 tetrahedra are in the middle of the layer, sandwiched by PO_3OH and $PO_2(OH)_2$ tetrahedra residing on the surface of the layers. A similar layer (Figure 9c) was found in the $Ti_2O_2H(PO_4)[(NH_4)_2PO_4]_2$,[16a] where TiO_6 octahedra are also in the middle. On the contrary, for the layer of $[Ti_2(PO_4)_2F_4]^{2-}$ (Figure 9d) in $Ti_2(PO_4)_2F_4 \cdot N_2C_2H_{10}$,[7f] TiO_2F_4 octahedra are located on the surface and the PO_4 tetrahedra are buried in the middle of the layer. The layer in $(H_3NC_2H_4NH_2)TiOPO_4$[16b] is different because it is electrically neutral and TiO_5N octahedra are connected directly by corner-sharing to

(14) Murugavel, R.; Kuppuswamy, S. *Angew. Chem., Int. Ed.* **2006**, *45*, 7022.

(15) (a) Isobe, T.; Watanabe, T.; de la Caillerie, J. B. D.; Legrand, A. P.; Massiot, D. *J. Colloid Interface Sci.* **2003**, *261*, 320–324. (b) Boysen, D. A.; Haile, S. M.; Liu, H. J.; Secco, R. A. *Chem. Mater.* **2003**, *15*, 727. (c) Yamada, K.; Sagara, T.; Yamane, Y.; Ohki, H.; Okuda, T. *Solid State Ionics* **2004**, *175*, 557. (d) Riou, D.; Fayon, F.; Massiot, D. *Chem. Mater.* **2002**, *14*, 2416.

(16) (a) Garcia-Granda, S.; Salvado, M. A.; Pertierra, P.; Garcia, J. R.; Bortun, A. I.; Clearfield, A. *Mater. Sci. Forum* **2001**, *378*−*381*, 665. (b) Zhao, Y. N.; Zhu, G. S.; Jiao, X. L.; Liu, W.; Pang, W. Q. *J. Mater. Chem.* **2000**, *10*, 463.

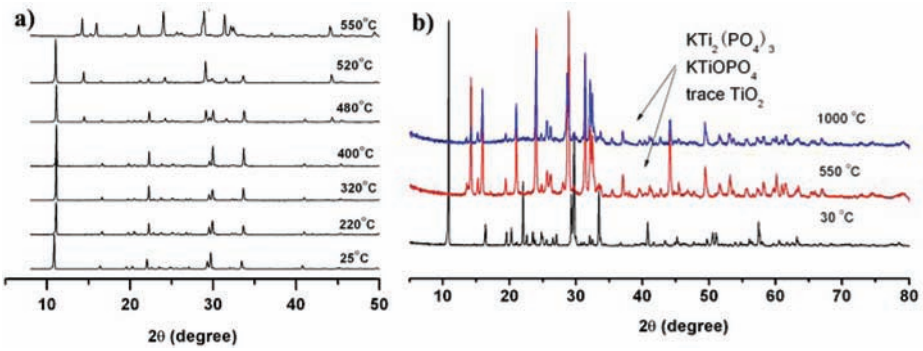

Figure 8. X-ray diffraction patterns of **1** treated at different temperatures.

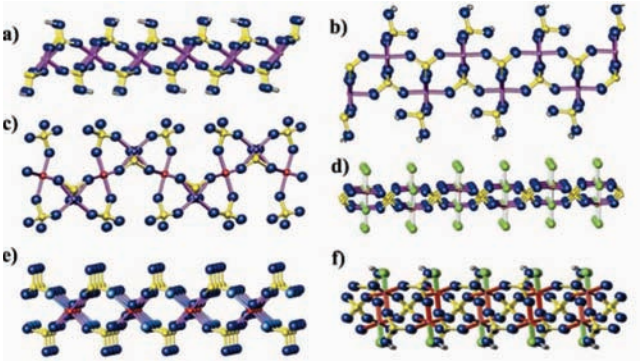

Figure 9. Typical layers for titanium phosphates: (a) α-$Ti(HPO_4)_2 \cdot H_2O$,[4] (b) γ-$Ti(H_2PO_4)(PO_4) \cdot 2H_2O$,[5] (c) $Ti_2O_2H(PO_4)[(NH_4)_2PO_4]_2$,[13a] (d) $Ti_2(PO_4)_2F_4 \cdot N_2C_2H_{10}$,[7f] (e) $(H_3NC_2H_4NH_2)TiOPO_4$,[13b] (f) $(NH_4)_{0.16}K_{1.84}[Ti_2F_2(PO_4)_2(PO_3OH)]$.

form chains. The layer of **1** prepared in this study is very unique in that both TiO_5F octahedra and PO_3OH tetrahedra are on the surface of the layer, which leads to two different hydrogen bondings involving both P−OH and Ti−F groups. Thus, this new material combines the properties of α-TiP, γ-TiP, and $[Ti_2(PO_4)_2F_4]^{2-}$. The TGA results show that the thermal stability of **1** is higher than that of α-, γ-, and β-TiP. It is stable up to 400 °C. The intercalation chemistry and surface catalytic properties of this new material are currently under investigation.

Acknowledgment. This work is supported by the National Natural Science Foundation of China (Grants 20771008, 2073116003, and 20821091). Y.H. thanks the NSERC of Canada for funding.

Supporting Information Available: CIF file of the structure reported in this paper, atomic parameters of **1**, $^{31}P\{^{19}F\}$ REDOR spectra of **1**, and a comparison of the different layers in several representative titanium phosphates. This material is available free of charge via the Internet at http://pubs.acs.org.